# Photoelectric converters with quantum coherence

Shan-He Su and Chang-Pu Sun*
*Beijing Computational Science Research Center, Beijing 100084, People's Republic of China*

Sheng-Wen Li
*Institute of Quantum Science and Engineering, Texas A&M University, College Station, Texas 77843, USA*

Jin-Can Chen
*Department of Physics, Xiamen University, Xiamen 361005, People's Republic of China*
(Received 6 January 2016; published 2 May 2016)

Photon impingement is capable of liberating electrons in electronic devices and driving the electron flux from the lower chemical potential to higher chemical potential. Previous studies hinted that the thermodynamic efficiency of a nanosized photoelectric converter at maximum power is bounded by the Curzon-Ahlborn efficiency $\eta_{\mathrm{CA}}$. In this study, we apply quantum effects to design a photoelectric converter based on a three-level quantum dot (QD) interacting with fermionic baths and photons. We show that, by adopting a pair of suitable degenerate states, quantum coherences induced by the couplings of QDs to sunlight and fermion baths can coexist steadily in nanoelectronic systems. Our analysis indicates that the efficiency at maximum power is no longer limited to $\eta_{\mathrm{CA}}$ through manipulation of carefully controlled quantum coherences.

DOI: 10.1103/PhysRevE.93.052103

## I. INTRODUCTION

Carnot's theorem states that all real heat engines operating between two heat baths undergo irreversible processes and are less efficient than a reversible heat engine, regardless of the working substance used or the operation details. Numerous studies have attempted to design more efficient heat engines and improve the work extraction when quantum effects come into play [1–4]. Most of the quantum thermodynamic studies only emphasized achieving a conversion efficiency limit, which is inevitably accompanied by a vanishing power output [5,6]. More extensive research needs to be conducted regarding the interdependence of efficiency and power for practical applications. Based on the Newton heat transfer law, Curzon and Ahlborn found that the efficiency at maximum power of an endoreversible Carnot heat engine with irreversible heat transfer processes is given by $\eta_{\mathrm{CA}} = 1 - \sqrt{T_c/T_h}$, where $T_h$ is the temperature of the heat source and $T_c$ is the temperature of the heat sink [7]. Other various thermodynamic machines indicate that $\eta_{\mathrm{CA}}$ gives a good approximation for estimating the efficiency at maximum power [8–10]. In particular, Rutten *et al.* proved that the efficiency at maximum power of a nanosized photoelectric converter can be well predicted by the Curzon and Ahlborn efficiency [11]. Only in the case of the strong coupling condition between electron and heat flows and negligible nonradiative effects, can the efficiency more closely approach $\eta_{\mathrm{CA}}$.

An interesting question arises here: might quantum coherence survive stably in nanoelectronic systems and help to increase the efficiency at maximum power beyond the bound of the Curzon and Ahlborn efficiency? By considering a three-level quantum dot (QD) in thermal contact with two boson reservoirs, Li *et al.* confirmed that the interference of two transitions in a nonequilibrium environment can give rise to nonvanishing steady quantum coherence [12]. Noise-induced coherence is capable of breaking the detailed balance condition and enhancing the laser power of a quantum heat engine [13,14]. The efficiency at maximum power of the laser quantum heat engine has been shown to depend on the proper adjustment of the coherence parameters [15,16]. In these previous studies, the interaction between quantum systems and bosonic baths plays a key role in generating coherence. However, whether an electronic system in a fermionic environment enables the realizations of steady coherence and performance improvement is rarely discussed.

In this paper, in order to show that coherent transitions induced by the couplings of QDs to sunlight and fermion baths can coexist to promote the potential of light harvesting, we propose an experimentally feasible model of a nanophotoelectric converter. We will focus on the condition to effectively increase the efficiency at maximum power beyond the bound of Curzon-Ahlborn efficiency. The contents are organized as follows: In Sec. II, the general model of the converter is briefly described. In Sec. III, the motion equation of the QD is analytically computed. In Sec. IV, the thermodynamic quantities at steady state are derived. In Sec. V, the performance characteristics of the photoelectric converter are revealed by numerical calculation.

## II. GENERAL DESCRIPTION OF THE MODEL

The system schematic (Fig. 1) of a photoelectric converter consists of a three-level QD contacted by two fermionic baths and photons. The three-level QD is modeled by the Hamiltonian

$$H_S = \sum_{i=g_1,g_2,e,0} \varepsilon_i |i\rangle\langle i|, \tag{1}$$

with $|0\rangle$ being the state for no electron in the QD. $|g_1\rangle$, $|g_2\rangle$, and $|e\rangle$ represent one-electron states in levels $\varepsilon_{g_1}$, $\varepsilon_{g_2}$, and $\varepsilon_e$,

*cpsun@csrc.ac.cn

 

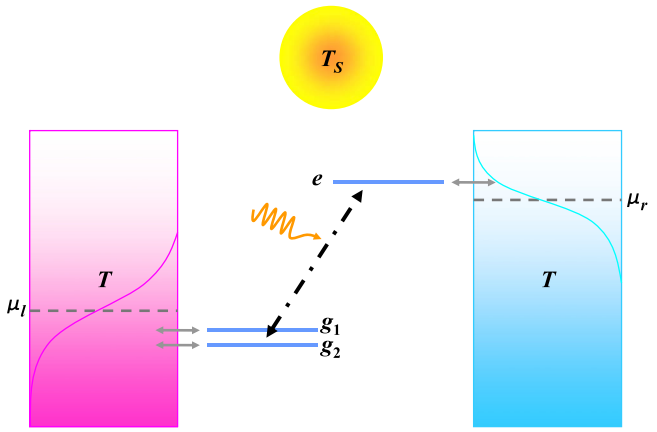


FIG. 1. Schematic of a photoelectric converter composed of a three-level QD. The degenerate ground states $|g_1\rangle$ and $|g_2\rangle$ are coupled to the left-fermionic bath, while the excited state $|e\rangle$ is coupled to the right-fermionic bath. The two fermionic baths are maintained at the same temperature $T$ but have different chemical potentials $\mu_l$ and $\mu_r = \mu_l + qV$ due to the applied voltage ($q$ is the elementary charge). Transitions between the ground states and the excited state are induced by photons with temperature $T_S$ (curved arrow).

respectively. We assume that Coulomb repulsions prevent two electrons from being simultaneously present in the QD [17]. One electron is first transferred from the left-fermionic bath to the ground state $|g_1\rangle$ or $|g_2\rangle$ via the QD-bath coupling, and then has a probability of being pumped to the excited state $|e\rangle$ due to the incoming solar radiation. The excited state $|e\rangle$ is coupled to the fermionic bath characterized by temperature $T$ and chemical potential $\mu_r$.

The Hamiltonian of the sunlight radiation ($R_P$) is given by

$$H_P = \sum_{k\in R_P} \omega_k a_k^\dagger a_k, \tag{2}$$

where $\omega_k$ is the eigenfrequency of the radiated electromagnetic wave described by the creation (annihilation) operator $a_k^\dagger$ ($a_k$). Similarly, the Hamiltonians of the fermionic baths ($R_l$ and $R_r$) are given by

$$H_F^{l,r} = \sum_{v\in R_{l,r}} \omega_v c_v^\dagger c_v. \tag{3}$$

Here, $c_v^\dagger$ ($c_v$) is the electron creation (annihilation) operator of the mode $\omega_v$ in $R_l$ or $R_r$. The two fermionic baths stand for the $n$- and $p$-type semiconductor electrodes of the photoelectric converter.

The interaction between the QD and the environment reads $H_I = H_I^l + H_I^r + H_I^P$ with each term defined by

$$H_I^l = \sum_{i=1,2}\sum_{v\in R_l} (T_{v_i} c_v |g_i\rangle\langle 0| + \text{H.c.}), \tag{4}$$

$$H_I^r = \sum_{v\in R_r} (T_{v_e} c_v |e\rangle\langle 0| + \text{H.c.}), \tag{5}$$

and

$$H_I^P = \sum_{i=1,2}\sum_{k\in R_P} (g_{k_i} a_k |e\rangle\langle g_i| + \text{H.c.}), \tag{6}$$

where $T_{v_i}$, $T_{v_e}$, and $g_{k_i}$ denote the coupling strength of the transitions between the QD and the left-fermionic bath, the right-fermionic bath, and photons, respectively.

## III. MOTION EQUATION OF THE QUANTUM DOT

The three-level QD can be viewed as an open quantum system vulnerable to interactions with the environment. Making the Born-Markov approximation, which involves assuming that the environment is time independent and the environment correlations decay rapidly in comparison to the typical time scale of the system evolution [18], we derive the equation of motion for the density operator $\rho$ in a Lindblad-like form

$$\dot\rho = i[\rho, H_S] + \mathcal{L}_P[\rho] + \mathcal{L}_l[\rho] + \mathcal{L}_r[\rho]. \tag{7}$$

The dissipative part in the master equation can be generalized into three individual elements including the dampings through the photons and the two fermionic baths. For the photon excitation, the dissipation operator $\mathcal{L}_P[\rho]$ depends on the Bose-Einstein statistics of the photons and is given by

$$\begin{aligned}\mathcal{L}_P[\rho] = i[\rho, H_{CP}] + \sum_{i,j=1}^{2} \Big\{ &[B_{ij}^+(\varepsilon_j) + B_{ij}^+(\varepsilon_i)] \\ &\times \Big[\sigma_{Pi}^\dagger \rho \sigma_{Pj} - \frac{1}{2}\{\rho, \sigma_{Pj}\sigma_{Pi}^\dagger\}_+\Big] + [B_{ji}^-(\varepsilon_j) + B_{ji}^-(\varepsilon_i)] \\ &\times \Big[\sigma_{Pi}\rho\sigma_{Pj}^\dagger - \frac{1}{2}\{\rho, \sigma_{Pj}^\dagger\sigma_{Pi}\}_+\Big]\Big\},\end{aligned} \tag{8}$$

where $\sigma_{Pi} = |g_i\rangle\langle e|$, $B_{ij}^+(\varepsilon_j) = \gamma_{ij}^P(\varepsilon_j) n(x_j)$, and $B_{ij}^-(\varepsilon_j) = \gamma_{ij}^P(\varepsilon_j)[1 + n(x_j)]$ are the dissipation rates with $\gamma_{ij}^P(\omega) = \pi \sum g_{k_i} g_{k_j}^* \delta(\varepsilon - \omega) = [\gamma_{ji}^P(\omega)]^*$; $n(x) = [\exp(x) - 1]^{-1}$ is the Bose-Einstein distribution with scaled energy $x_j = \varepsilon_j/(k_B T_P)$ and $k_B$ is the Boltzmann constant. The energy difference of each transition is defined as $\varepsilon_j = \varepsilon_e - \varepsilon_{g_j}$. The left-fermionic bath is coupled to the ground states $|g_1\rangle$ and $|g_2\rangle$. The corresponding dissipation operator is then expressed as

$$\begin{aligned}\mathcal{L}_l[\rho] = i[\rho, H_{Cl}] + \sum_{i,j=1}^{2} \Big\{ &\big[F_{ij}^{l+}(\varepsilon_{g_j}) + F_{ij}^{l+}(\varepsilon_{g_i})\big] \\ &\times \Big[\sigma_{li}^\dagger \rho \sigma_{lj} - \frac{1}{2}\{\rho, \sigma_{lj}\sigma_{li}^\dagger\}_+\Big] + [F_{ji}^{l-}(\varepsilon_{g_j}) + F_{ji}^{l-}(\varepsilon_{g_i})] \\ &\times \Big[\sigma_{li}\rho\sigma_{lj}^\dagger - \frac{1}{2}\{\rho, \sigma_{lj}^\dagger\sigma_{li}\}_+\Big]\Big\},\end{aligned} \tag{9}$$

where $\sigma_{li} = |0\rangle\langle g_i|$, $F_{ij}^{l+}(\varepsilon_{g_j}) = \gamma_{ij}^l(\varepsilon_{g_j}) f(x_{g_j})$, and $F_{ij}^{l-}(\varepsilon_{g_j}) = \gamma_{ij}^l(\varepsilon_{g_j})[1 - f(x_{g_j})]$ with $\gamma_{ij}^l(\omega) = \pi \sum T_{v_i} T_{v_j}^* \delta(\varepsilon - \omega) = [\gamma_{ji}^l(\omega)]^*$; $f(x) = [\exp(x) + 1]^{-1}$ is the Fermi distribution with scaled energies of the ground states $x_{g_j} = (\varepsilon_{g_j} - \mu_l)/(k_B T)$. The dissipation operator describes the coupling between the right-fermionic bath and the excited state as

$$\begin{aligned}\mathcal{L}_r[\rho] = &F^{r+}(\varepsilon_e)[2\sigma_{re}^\dagger \rho \sigma_{re} - \sigma_{re}\sigma_{re}^\dagger \rho - \rho\sigma_{re}\sigma_{re}^\dagger] \\ &+ F^{r-}(\varepsilon_e)[2\sigma_{re}\rho\sigma_{re}^\dagger - \sigma_{re}^\dagger\sigma_{re}\rho - \rho\sigma_{re}^\dagger\sigma_{re}],\end{aligned} \tag{10}$$

where $\sigma_{re} = |0\rangle\langle e|$. $F^{r+}(\varepsilon_e) = \gamma^r(\varepsilon_e) f(x_r)$ and $F^{r-} = \gamma^r(\varepsilon_e)[1 - f(x_r)]$ with $\gamma^r(\omega) = \pi \sum T_{v_e} T^*_{v_e} \delta(\varepsilon - \omega) = [\gamma^r(\omega)]^*$. $x_r = (\varepsilon_e - \mu_r)/(k_B T)$ is the scaled energy of the excited state.

Notice that the interference of coherent transitions can be simultaneously induced by the photons and the left-fermionic bath, leading to two different nondiagonal couplings given by

$$H_{CP} = \frac{1}{2i} \sum_{i,j=1}^{2} \{[B^+_{ij}(\varepsilon_i) - B^+_{ij}(\varepsilon_j)]\sigma_{Pj}\sigma^\dagger_{Pi} + [B^-_{ji}(\varepsilon_i) - B^-_{ji}(\varepsilon_j)]\sigma^\dagger_{Pj}\sigma_{Pi}\} \tag{11}$$

and

$$H_{Cl} = \frac{1}{2i} \sum_{i,j=1}^{2} \left\{\left[F^{l+}_{ij}(\varepsilon_{g_i}) - F^{l+}_{ij}(\varepsilon_{g_j})\right]\sigma_{lj}\sigma^\dagger_{li} + \left[F^{l-}_{ji}(\varepsilon_{g_i}) - F^{l-}_{ji}(\varepsilon_{g_j})\right]\sigma^\dagger_{lj}\sigma_{li}\right\}. \tag{12}$$

According to Eqs. (7)—(10), we have a coupled set of equations describing the dynamics of the populations, $\rho_i = \langle g_i|\rho|g_i\rangle$, $\rho_e = \langle e|\rho|e\rangle$, $\rho_0 = \langle 0|\rho|0\rangle$, and the coherence, $\rho_{ij} = \langle g_i|\rho|g_j\rangle$, as follows:

$$\dot\rho_1 = -2\left[B^+_{11}(\varepsilon_1) + F^{l-}_{11}(\varepsilon_{g_1})\right]\rho_1 + 2B^-_{11}(\varepsilon_1)\rho_e + 2F^{l+}_{11}(\varepsilon_{g_1})\rho_0 - \left[B^+_{12}(\varepsilon_2) + F^{l-}_{21}(\varepsilon_{g_2})\right]\rho_{12} - \left[B^+_{21}(\varepsilon_2) + F^{l-}_{12}(\varepsilon_{g_2})\right]\rho_{21}, \tag{13}$$

$$\dot\rho_2 = -2\left[B^+_{22}(\varepsilon_2) + F^{l-}_{22}(\varepsilon_{g_2})\right]\rho_2 + 2B^-_{22}(\varepsilon_2)\rho_e + 2F^{l+}_{22}(\varepsilon_{g_2})\rho_0 - \left[B^+_{12}(\varepsilon_1) + F^{l-}_{21}(\varepsilon_{g_1})\right]\rho_{12} - \left[B^+_{21}(\varepsilon_1) + F^{l-}_{12}(\varepsilon_{g_1})\right]\rho_{21}, \tag{14}$$

$$\begin{aligned}\dot\rho_e = {} & 2B^+_{11}(\varepsilon_1)\rho_1 + 2B^+_{22}(\varepsilon_2)\rho_2 - 2[B^-_{11}(\varepsilon_1) + B^-_{22}(\varepsilon_2) + F^{r-}(\varepsilon_e)]\rho_e + 2F^{r+}(\varepsilon_e)\rho_0 + [B^+_{12}(\varepsilon_1) + B^+_{12}(\varepsilon_2)]\rho_{12} \\ & + [B^+_{21}(\varepsilon_1) + B^+_{21}(\varepsilon_2)]\rho_{21},\end{aligned} \tag{15}$$

$$\begin{aligned}\dot\rho_0 = {} & 2F^{l-}_{11}(\varepsilon_{g_1})\rho_1 + 2F^{l-}_{22}(\varepsilon_{g_2})\rho_2 + 2F^{r-}(\varepsilon_e)\rho_e - 2\left[F^{l+}_{11}(\varepsilon_{g_1}) + F^{l+}_{22}(\varepsilon_{g_2}) + F^{r+}(\varepsilon_e)\right]\rho_0 + \left[F^{l-}_{21}(\varepsilon_{g_1}) + F^{l-}_{21}(\varepsilon_{g_2})\right]\rho_{12} \\ & + \left[F^{l-}_{12}(\varepsilon_{g_1}) + F^{l-}_{12}(\varepsilon_{g_2})\right]\rho_{21},\end{aligned} \tag{16}$$

and

$$\begin{aligned}\dot\rho_{12} = {} & -\left[B^+_{21}(\varepsilon_1) + F^{l-}_{12}(\varepsilon_{g_1})\right]\rho_1 - \left[B^+_{21}(\varepsilon_2) + F^{l-}_{12}(\varepsilon_{g_2})\right]\rho_2 + [B^-_{21}(\varepsilon_1) + B^-_{21}(\varepsilon_2)]\rho_e + \left[F^{l+}_{12}(\varepsilon_{g_1}) + F^{l+}_{12}(\varepsilon_{g_2})\right]\rho_0 \\ & - \left[B^+_{11}(\varepsilon_1) + B^+_{22}(\varepsilon_2) + F^{l-}_{11}(\varepsilon_{g_1}) + F^{l-}_{22}(\varepsilon_{g_2}) + \tau\right]\rho_{12} + i\Delta_{21}\rho_{12}.\end{aligned} \tag{17}$$

Here, $\Delta_{21} = \varepsilon_{g_2} - \varepsilon_{g_1}$ is the energy difference of the two lower states $|g_1\rangle$ and $|g_2\rangle$, and $\tau$ is phenomenologically introduced to describe the decoherence rate due to the environment effects. The equations for off-diagonal terms, e.g., $\langle g_i|\rho|e\rangle$ and $\langle e|\rho|0\rangle$, have been omitted except $\rho_{12}$, since those terms only give the decay processes and do not affect the steady-state solution. It is shown that the time evolutions of the populations $\rho_i$, $\rho_e$, and $\rho_0$ are not decoupled from that of the off-diagonal elements $\rho_{12}/\rho_{21}$. The coherence $\rho_{12}/\rho_{21}$ may not vanish even in the steady state after long time evolution. Specifically, we find that both QD-photon coupling and QD-fermion coupling contribute to the coherent transitions.

## IV. THERMODYNAMIC QUANTITIES AT STEADY STATE

For degenerate lower levels $\varepsilon_{g_1} = \varepsilon_{g_2} = \varepsilon_l$ and symmetric couplings, we write the rates of transitions $|g_1\rangle \leftrightarrow |e\rangle$ and $|g_2\rangle \leftrightarrow |e\rangle$ as $\gamma^P_{11}(\varepsilon_1) = \gamma^P_{22}(\varepsilon_2) = \gamma^P$ and that of transitions $|g_1\rangle \leftrightarrow |0\rangle$ and $|g_2\rangle \leftrightarrow |0\rangle$ as $\gamma^l_{11}(\varepsilon_{g_1}) = \gamma^l_{22}(\varepsilon_{g_2}) = \gamma^l$. We also introduce two dimensionless parameters $r_P(= \gamma^P_{12}/\gamma^P)$ and $r_l(=\gamma^l_{12}/\gamma^l)$ to describe the strengths of coherences, where superscripts $P$ and $l$ imply the coherent transitions originating from the couplings to the photons and the left-fermionic bath, respectively. Note that $0 \leqslant r_P,\ r_l \leqslant 1$, depending on the relative orientations of transition dipole vectors [15]. Setting $\dot\rho = 0$ and combining Eqs. (13)–(17) with the conservative equation $\rho_1 + \rho_2 + \rho_e + \rho_0 = 1$, the steady-state populations and coherence of the open quantum system are obtained. The coherence is computed as

$$\begin{aligned}\rho_{12} = {} & 2\gamma^P(r_P - r_l)\{n(x_g)f(x_l) - [1 + n(x_g) \\ & - f(x_l)]f(x_r)\}/\Omega,\end{aligned} \tag{18}$$

where $\Omega$ is the normalization factor that ensures the sum of probabilities to be equal to unity. Simplifying the numerator of Eq. (18) to $1/2\gamma^P(r_l - r_P)\mathrm{csch}(x_g/2)\mathrm{sech}(x_l/2)\mathrm{sech}(x_r/2)\sinh[(x_g + x_l - x_r)/2)]$, we identify that $\rho_{12}$ reduces to zero when $r_P = r_l$ and the quantum coherence will not affect the thermodynamics. This phenomenon was observed in a four-level quantum heat engine for the symmetric coupling condition as well [16].

From the master equation, the changing rate of the electron number in the three-level QD at time $t$ is

$$\dot{\overline{N}}(t) = \mathrm{Tr}\{n\mathcal{L}_l[\rho]\} + \mathrm{Tr}\{n\mathcal{L}_r[\rho]\} := J_l - J_r \tag{19}$$

with the number operator $n = \sigma^\dagger_{re}\sigma_{re} + \sigma^\dagger_{l1}\sigma_{l1} + \sigma^\dagger_{l2}\sigma_{l2}$. Thus, $J_l$ and $J_r$ are the currents exchanging with the left- and right-fermionic baths, which are given by

$$J_l = 4\gamma^l f(x_l)\rho_0 - 2\gamma^l[1 - f(x_l)]\{\rho_1 + \rho_2 + r_l\mathrm{Re}[\rho_{12}]\} \tag{20}$$

and

$$J_r = 2\gamma^r[1 - f(x_r)]\rho_e - 2\gamma^r f(x_r)\rho_0. \quad (21)$$

The parameter $x_l = (\varepsilon_l - \mu_l)/(k_B T)$ is the scaled energy of the degenerate ground states. In the stationary state ($t \to \infty$), $\dot{N}(t) = 0$ such that $J_l = J_r = J$. Equation (20) indicates that adjusting the electron current via quantum coherences allows for improving the performance of the converter. The steady-state energy fluxes are determined by the energy change of the three-level QD, i.e., $\dot{E}(\infty) = \mathrm{Tr}\{H_S\dot{\rho}(\infty)\} = \sum_\alpha \mathrm{Tr}\{H_S\mathcal{L}_\alpha[\rho(\infty)]\}$ ($\alpha = P, l$, and $r$). Neglecting the nonradiative recombination processes [11,19], the net heat flux coming from the sunlight $\dot{Q}_P = \mathrm{Tr}\{H_S\mathcal{L}_P[\rho(\infty)]\} = \varepsilon_g J$, where $\varepsilon_g = \varepsilon_e - \varepsilon_l$ can be regarded as the band-gap energy. The power $P$ generated by the photoelectric converter to move electrons from the left-fermionic bath to the right-fermionic bath yields

$$P = (\mu_r - \mu_l)J = k_B T_P[x_g - (1 - \eta_c)(x_r - x_l)]J \quad (22)$$

with $x_g = \varepsilon_g/(k_B T_P)$. The symbol $\eta_c$ denotes the Carnot efficiency and equals $1 - T/T_P$. The efficiency satisfying this conversion is then given by

$$\eta = \frac{P}{\dot{Q}_P} = \frac{(\mu_r - \mu_l)J}{\varepsilon_g J} = 1 - (1 - \eta_c)\frac{(x_r - x_l)}{x_g}. \quad (23)$$

The heat currents due to electron exchanges between the QD and the two fermionic baths are $\dot{Q}_l = \mathrm{Tr}\{H_S\mathcal{L}_l[\rho(\infty)]\} - \mu_l J = (\varepsilon_l - \mu_l)J$ and $\dot{Q}_r = \mathrm{Tr}\{H_S\mathcal{L}_r[\rho(\infty)]\} - \mu_r(-J) = -(\varepsilon_e - \mu_r)J$, respectively [20]. These formulas conveniently relate the heat currents to energy and matter currents from the fermionic baths into the QD. At steady state, the entropy of the converter remains constant. The entropy production in the QD must be positive and balanced by the entropy flow through its terminals [6,17,20]

$$R = -\left(\frac{\dot{Q}_P}{T_S} + \frac{\dot{Q}_l + \dot{Q}_r}{T}\right) = (x_r - x_l - x_g)k_B J. \quad (24)$$

.

## V. PERFORMANCE CHARACTERISTIC ANALYSIS

In the following section, we address the question regarding the extent to which the quantum nature of the converter affects the photoelectric conversion efficiency, a topic which is beyond the reach of the model presented in Ref. [11]. The formalism obtained here will allow us to access how coherences can lead to an enhancement of the power and the efficiency. To do so, we parametrize the transition rates $\gamma^P = \gamma^l = \gamma^r = \gamma$ without loss of generality.

Figures 2(a), 2(b), and 2(c) show the contour plots of the absolute value of coherence $|\rho_{12}|$, the efficiency $\eta$, and the entropy production rate $R/k_B$, respectively, versus $r_P$ and $r_l$, where the power has been optimized with respect to $x_l$ and $x_r$. In accordance with the requirements set out in the analytical method [Eq. (18)], Fig. 2(a) shows that the quantum coherence vanishes if $r_P = r_l$, resulting in a low efficiency less than 0.87. To enhance $\eta$ in the presence of coherence ($|\rho_{12}| \neq 0$), $r_P$ and $r_l$ should be designed to be different from each

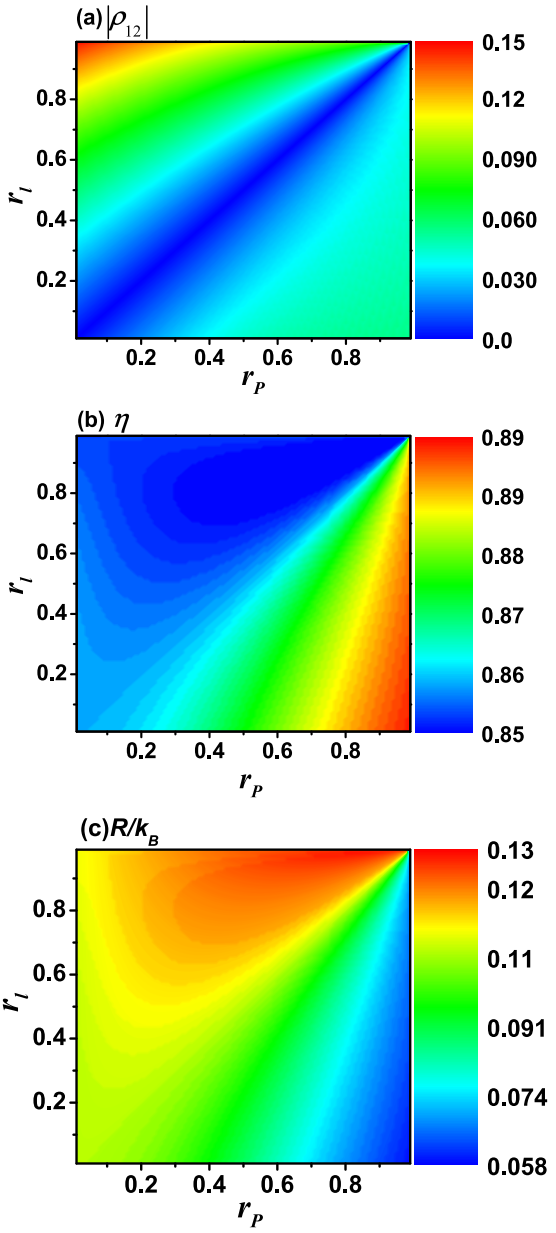


FIG. 2. The absolute value of coherence (a), the efficiency (b), and the entropy production rate divided by the Boltzmann constant (c) as a function of the dimensionless parameters $r_P$ and $r_l$, where $x_g = 2$, $\tau = 0$, $T = 295$ K, and $T_P = 5780$ K. The optimal values of $x_l$ and $x_r$ have been computed numerically to maximize the power output.

other. However, we notice that $\eta$ and $|\rho_{12}|$ may not always increase or decrease together, which means that $\eta$ is not only restricted by the magnitude of coherence. Comparing Fig. 2(a) with Fig. 2(b), we find that $\eta$ can be largely enhanced in the range of $r_P > r_l$. This condition suggests that increasing the coherence coupling between the QD and the photons and $|\rho_{12}|$ will concurrently benefit the performance of the photoelectric conversion. There exists a perfect positive correlation between $\eta$ and $|\rho_{12}|$ when $r_P > r_l$ is satisfied. Figure 2(c) indicates that the entropy production rate always remains positive without violating the second law of thermodynamics. The irreversible

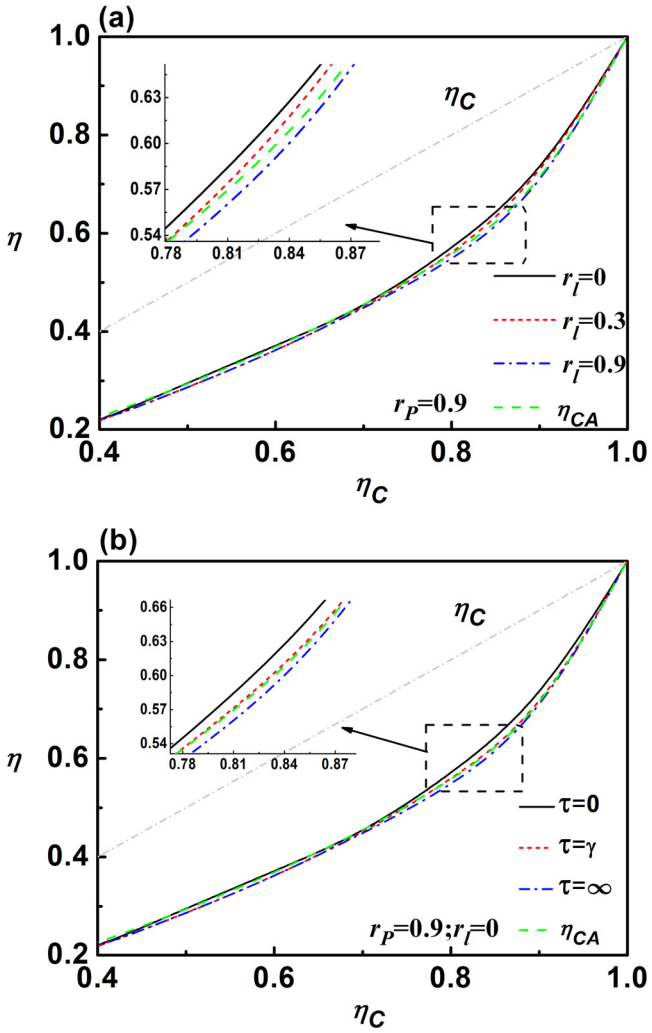


FIG. 3. The efficiency at maximum power and the Curzon-Ahlborn efficiency (green dashed line) as a function of Carnot efficiency $\eta_c$ for different values of $r_l$ (a) and $\tau$ (b). In Fig. 3(a), $r_P = 0.9$ and $\tau = 0$. In Fig. 3(b), $r_P = 0.9$ and $r_l = 0$. The inset figure shows an enlargement of the representative part of each plot.

entropy production rate has a lower value in the region of $r_P > r_l$.

Next, we maximize the power with respect to $x_g$, $x_l$, and $x_r$. In Fig. 3(a), the efficiency at maximum power is plotted as a function of $\eta_c$ for given values of $r_P$. Figure 3(a) shows that the efficiency at maximum power increases with a decrease in the parameter $r_l$, as expected. When $r_P = r_l = 0.9$ (dash-dotted line), the efficiency remains close to the Curzon-Ahlborn efficiency for almost all values of $\eta_c$. Slightly lower efficiencies are observed only far from equilibrium where $\eta_c$ is large. These features have also been addressed in other approaches to nonequilibrium thermodynamics, such as a Brownian heat engine [21,22], a Feynman ratchet model [23], and a thermoelectric device [24], and therefore point to a fundamental principle that can be associated with the presence of inherently irreversible dynamics when the device is operated at maximum power.

Intriguingly, we find that the efficiency at maximum power is not limited by the Curzon-Ahlborn efficiency. For example, when $r_l = 0.3$ (short-dashed line) or $r_l = 0$ (solid line), the quantum coherence appears and the efficiency at maximum power will exceed the bound given by the Curzon-Ahlborn efficiency. These results are remarkable in our model with quantum coherence. The quantum coherence will redistribute the population in the three-level QD and accelerate the removal of electrons, thus increasing the number of absorbed photons and reducing recombination losses.

Finally, we consider the typical problem arising due to the decoherence. Decoherence occurs when a system interacts with its environment in a thermodynamically irreversible way. The decoherence processes can drastically decrease an engine's efficiency. In Fig. 3(b), the efficiency at maximum power is plotted as a function of $\eta_c$ with $r_P = 0.9$ and $r_l = 0$. In the case that the decoherence rate is extremely large, i.e., $\tau \to \infty$, the efficiency (dashed line) again becomes slightly lower than the Curzon-Ahlborn efficiency. As $\tau$ diminishes, we find that the efficiency increases monotonically. The efficiency at maximum power is significantly higher than the Curzon-Ahlborn efficiency when $\tau = 0$.

## VI. CONCLUSIONS

In summary, we propose a type of photoelectric converter which consists of a three-level QD coupling to two fermionic baths and sunlight radiation. It follows from the Born-Markov approximation that the interference due to coherent transitions can be simultaneously induced by the sunlight and the left-fermionic bath, leading to two different nondiagonal Lamb shifts in the Lindblad-like master equation. The results of the thermodynamic analysis show that the quantum coherence is capable of improving the efficiency beyond the limit of a system whose quantum effects are absent. The application of quantum mechanics will bring new insight into understanding the fundamental problem in thermodynamics when it is applied to nanoelectronic systems.

## ACKNOWLEDGMENTS

This work has been supported by the National Natural Science Foundation of China (Grants No. 11421063 and No. 11534002), the National 973 program (Grants No. 2012CB922104 and No. 2014CB921403), and the Postdoctoral Science Foundation of China (Grant No. 2015M580964).

[1] M. O. Scully, M. S. Zubairy, G. S. Agarwal, and H. Walther, Science **299**, 862 (2003).

[2] J. Roßnagel, O. Abah, F. Schmidt-Kaler, K. Singer, and E. Lutz, Phys. Rev. Lett. **112**, 030602 (2014).

[3] X. L. Huang, Tao Wang, and X. X. Yi, Phys. Rev. E **86**, 051105 (2012).

[4] H. T. Quan, P. Zhang, and C. P. Sun, Phys. Rev. E **73**, 036122 (2006).

[5] R. S. Whitney, Phys. Rev. Lett. **112**, 130601 (2014).
[6] M. Esposito, R. Kawai, K. Lindenberg, and C. Van den Broeck, Phys. Rev. Lett. **105**, 150603 (2010).
[7] F. L. Curzon and B. Ahlborn, Am. J. Phys. **43**, 22 (1975).
[8] J. Wang, Z. Ye, Y. Lai, W. Li, and J. He, Phys. Rev. E **91**, 062134 (2015).
[9] F. Wu, J. He, Y. Ma, and J. Wang, Phys. Rev. E **90**, 062134 (2014).
[10] J. Guo, J. Wang, Y. Wang, and J. Chen, Phys. Rev. E **87**, 012133 (2013).
[11] B. Rutten, M. Esposito, and B. Cleuren, Phys. Rev. B **80**, 235122 (2009).
[12] S. W. Li, C. Y. Cai, and C. P. Sun, Ann. Phys. (NY) **360**, 19 (2015).
[13] M. O. Scully, K. R. Chapin, K. E. Dorfman, M. B. Kim, and A. Svidzinsky, Proc. Natl. Acad. Sci. USA **108**, 15097 (2011).
[14] K. E. Dorfman, D. V. Voronine, S. Mukamel, and M. O. Scully, Proc. Natl. Acad. Sci. USA **110**, 2746 (2013).
[15] U. Harbola, S. Rahav, and S. Mukamel, Europhys. Lett. **99**, 50005 (2012).
[16] H. P. Goswami and U. Harbola, Phys. Rev. A **88**, 013842 (2013).
[17] B. Cleuren, B. Rutten, and C. Van den Broeck, Phys. Rev. Lett. **108**, 120603 (2012).
[18] H. P. Breuer and F. Petruccione, *The Theory of Open Quantum Systems* (Oxford University Press, Oxford, 2001).
[19] J. Wang, Y. Lai, Z. Ye, J. He, Y. Ma, and Q. Liao, Phys. Rev. E **91**, 050102(R) (2015).
[20] G. Schaller, *Open Quantum Systems Far from Equilibrium* (Springer, New York, 2014).
[21] V. Blickle and C. Bechinger, Nat. Phys. **8**, 143 (2012).
[22] Z. C. Tu, Phys. Rev. E **89**, 052148 (2014).
[23] Z. C. Tu, J. Phys. A **41**, 312003 (2008).
[24] M. Esposito, K. Lindenberg, and C. Van den Broeck, Europhys. Lett. **85**, 60010 (2009).